Surface Science 237 (1990) 257–265
North-Holland

Coadsorption of Cs and hydrogen on W(110) studied by metastable impact electron spectroscopy

W. Maus-Friedrichs, M. Wehrhahn, S. Dieckhoff and V. Kempter
Physikalisches Institut der TU Clausthal, 3392 Clausthal-Zellerfeld, Fed. Rep. of Germany

Received 18 April 1990; accepted for publication 6 July 1990

The adsorption of hydrogen and Cs alone as well as the coadsorption of Cs and hydrogen on W(110) was studied by metastable impact electron spectroscopy (MIES) and supplemented by UPS, AES, and work function measurements. The main conclusions are: (a) ionization of the Cs(6s) level is not observed for Cs coverages $\theta_{Cs} \leq 0.4$ ML, (b) the formation of a H(1S)–metal bond occurs at a binding energy of $E_B = 4.7$ eV, (c) upon Cs and hydrogen coadsorption an independent layer of hydrogen is formed between the substrate and the Cs adlayer. The charge density of the Cs adlayer is lowered by about 25% upon the formation of the hydrogen intermediate layer.

1. Introduction

A detailed study of the coadsorption of hydrogen and Cs on W(110) using the standard techniques LEED, AES, TDS, and work function (WF) measurements has been published recently [1]. The main conclusions were as follows:

- a layer of atomic hydrogen is formed between the substrate and the Cs adlayer,
- Cs forms an independent layer above the hydrogen layer,
- H-preadsorption restricts the electronic interaction between the Cs adlayer and the substrate,
- the initial dipole moment and the electron density of the Cs overlayer are increased compared to that of the Cs layer without hydrogen preadsorption for all Cs coverages.

*M*etastable *I*mpact *E*lectron *S*pectroscopy (MIES) is uniquely suited to study the electronic structure of the outermost adlayer at surfaces [2]. We prefer the acronym MIES rather than MDS (*M*etastable *D*eexcitation *S*pectroscopy) for the reasons given in ref. [3]. Applied to the coadsorption of hydrogen and cesium on W(110) and based on the conclusions summarized above the deexcitation of metastable noble gas atoms leads to the following picture:

- as for the adsorption of Cs alone the MIES spectrum should essentially consist of three peaks due to the ionization of Cs(6s) and Cs($5p_{1/2,3/2}$) by the metastable He atoms. Deexcitation of the He atoms is restricted to the Cs toplayer. No hydrogen induced features should appear,
- the degree of metallization in the Cs overlayer is reflected in the ratio of the peak intensities for ionization of Cs(6s) and Cs($5p_{3/2,1/2}$). Therefore an increase of the metallization of the Cs adlayer due to hydrogen preadsorption should manifest itself in an increase of this peak ratio with increasing hydrogen precoverage,
- possible changes of the bandwidth of the two-dimensional Cs adlayer caused by H-preadsorption should influence the width of the Cs(6s) peak.

We have studied the Cs adsorption both on clean and hydrogen precovered W(110) by MIES. In addition, hydrogen adsorption on clean W(110) was also followed by MIES observing the electron emission due to the *A*uger *N*eutralization (AN) process and UPS. AES and WF measurements have been carried out in order to relate our results to those of Papageorgopoulos [1]. MIES results

are supplemented by UPS measurements performed with the same excitation source which has been employed to produce the metastable noble gas beam.

2. Experimental

The measurements have been carried out in an ion-pumped standard apparatus for surface diagnosis (model TNB-X of Perkin Elmer) which is bakeable up to 180°C. The base pressure obtained using the ion pump supported by a LN_2 cooled sublimation pump is below 2×10^{-11} Torr. Additional pumping is provided by a Varian turbomolecular pump (type V450A, 450 ℓ/s) during MIES and UPS measurements.

The system consists of a cylindrical mirror analyzer (model 10-155 of Perkin-Elmer), a four grid LEED optics (model 15-120 of Perkin-Elmer), an electron gun for WF measurements (diode method), a hemispherical 180° analyzer (VSW model HA100), a quadrupole mass spectrometer (Extranuclear model 270-9) used for residual gas analysis, and the source for production of the thermal metastable He atoms.

The W(110) crystal can be heated up to 2500 K; its temperature is measured by a W/Rh–W thermocouple. Cleaning of the crystal is performed by the standard method of heating at 1400 K in 2×10^{-7} Torr O_2 and intermediate flashing up to 2500 K causing desorption of CO.

Alkali atoms are deposited onto the cleaned W(110) crystal from a SAES Getters source. The degree of coverage θ_{Cs} is estimated by following the ratio of the Cs(564 eV) and the W(350 eV) peaks. All measurements presented here have been performed at room temperature. At this temperature only one layer of Cs can be deposited onto the substrate, corresponding to a Cs density of $(5.2 \pm 0.3) \times 10^{14}$ cm^{-2}. In conformity with many authors we give the degree of coverage in fraction of the completed Cs adlayer which is denoted with 1 ML.

Hydrogen admission is made through a bakeable stainless steel gas inlet system through a precisely controlled leak valve. The gas admission system is baked out in regular time intervals. The purity of the admitted gas is monitored by means of the quadrupole mass spectrometer.

The He* source is schematically shown in fig. 1. The source is of the type described in ref. [4]

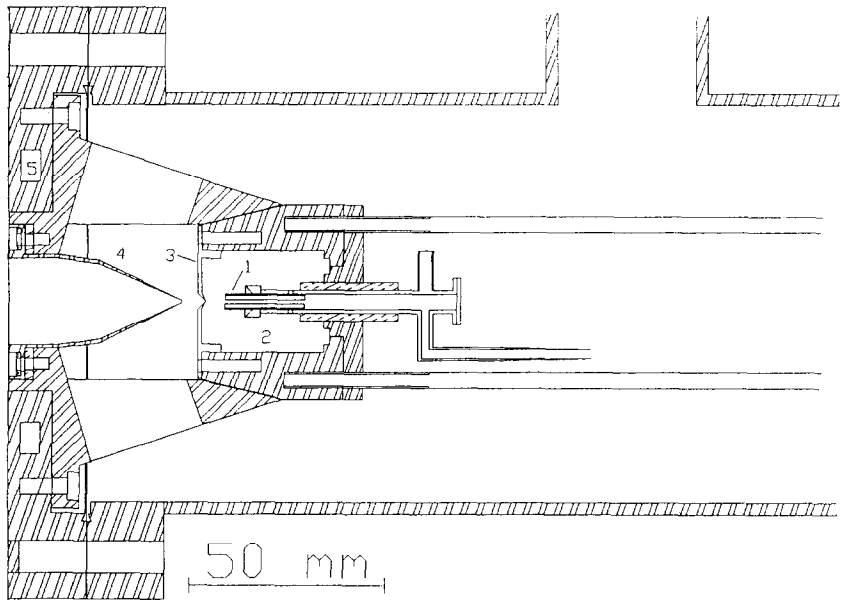

Fig. 1. Scheme of the source for MIES: 1 – cathode, 2 – excitation chamber, 3 – anode, 4 – skimmer, 5 – water cooling.

modified for operation in an UHV system. Its properties are essentially as described in refs. [3–5]. Metastable He* atoms are produced in a cold cathode DC discharge (340 V, 40 mA) source between cathode (1) and anode (3) operated at a pressure of about 0.5 Torr. The cathode (1) is made of molybdenum with an opening for the He inlet. The anode (1) is made of stainless steel and is grounded. The distance between cathode and anode may be changed; usually 4.5 mm are used. The source is formed conically to achieve easy mounting. The source is water cooled; the equipment for cooling is part of the device for positioning the source. A more detailed description can be found in ref. [6]. Both metastable inert gas atoms and UV photons are produced in the discharge. Some of them escape from the discharge region through a 0.4 mm aperture in (3), pass the skimmer (opening diameter 1 mm) (4), and finally enter the high vacuum region. The main function of the skimmer is pressure reduction behind the discharge region, lowering the pressure as quickly as possible to a value where the quenching of the metastables becomes negligible. The source chamber is pumped by a Varian turbomolecular pump (type V450A, 450 ℓ/s). The base pressure is below 10^{-6} Torr and the working pressure reaches 10^{-3} Torr. Between the source and the UHV chamber a buffer chamber is installed operating at a base pressure of 5×10^{-8} Torr and a working pressure of about 2×10^{-6} Torr. It is pumped with a Leybold TurboVac50 (50 ℓ/s). Furthermore a leak valve allows the inlet of inert gases like He or Ar. This option is used to quench all metastables out of the beam thus retaining only the UV photons in the beam and allowing to obtain UP-spectra. The He* ($2\,^3S$; $2\,^1S$) beam current density is about 5×10^{14} atoms/sr. The average beam velocity corresponds to a source temperature of 400 K [5]. The source produced both metastable species $2\,^3S$ and $2\,^1S$. We expect their relative intensity to be quite similar to that found in ref. [4], namely $He(2\,^3S) : He(2\,^1S) = 7 : 1$ because the modifications in the source design as compared to ref. [4] were only made with the purpose of operation under UHV conditions. However, the precise intensity ratio is of no importance for the interpretation of the results of our work. The He* source and the UHV chamber may be separated by a valve which is used while performing work function (WF) or AES measurements.

All measurements have been performed with the specimen under 45° both with respect to the incoming He* and the optical axis of the electron analyzer. The cleanness of the target has been monitored using AES, but the best method is MIES itself. No contamination of the target due to the He beam could be detected. The measurements have been carried out with a mixed beam containing both $He(2\,^3S)$ and $He(2\,^1S)$ atoms. As will be shown below most of the $He(2\,^1S)$ atoms are converted into $He(2\,^3S)$ prior to their deexcitation into the ground state [7,11]. Spectra have been recorded using the hemispherical analyzer (HA) controlled by a LEO AT computer equipped with an ORTEC EG&G *M*ultichannel *S*caling *C*ard (MCS) in pulse counting mode. Resolution of the HA has been 250 meV FHWM at a pass energy of 10 eV. WF measurements are conducted with the same computer using a DAC (*D*igital *A*nalog *C*onverter) and an ADC (*A*nalog *D*igital *C*onverter) in connection with software for compensation of the current variations. Collected data may be differentiated, smoothed, and plotted using another LEO AT and an IBM 3090 Host.

As has been demonstrated by Sesselmann et al. [8] variations of the SDOS (*S*urface *D*ensity *O*f *S*tates) as a function of the binding energy are reliably approximated by the first derivative of the AN-spectra. All deconvoluted spectra presented in this paper are obtained in this manner.

The count rates of MIES spectra are typically 10^2 times those of the UPS spectra.

3. Results

The spectra shown in figs. 2, 4 and 5 have been recorded using the following procedure:

(1) Cesium has been offered continuously at a small rate. The time required to complete and save one spectrum is about 40 s. We generally choose a rate high enough to complete a monolayer of Cs before the occurrence of residual gas features. The sensitivity of MIES is extremely high: we estimate

the oxygen coverage in fig. 5 to be less than 0.02 ML. The time required to take the entire set of spectra in figs. 4 or 5 amounts to about 12 min.

(2) During the studies of hydrogen adsorption a pressure of 8.3×10^{-9} Torr has been offered to the target, and spectra are recorded in time intervals of one minute. With clean metal surfaces He* deexcitation occurs via resonance ionization (RI) followed by Auger neutralization (AN). The maximum kinetic energy of the electrons emitted is given by

$$E_{max} = I - 2\phi,$$

where I is the effective ionization potential of the ground state of He and ϕ is the WF of the surface. An electron with E_{max} involves a second electron also originating from the Fermi level ($E_B = 0$). The position of the Fermi level is determined by the high-energy cut-off of the AN spectra at $E_{max} = 12.6$ eV. In UP emission induced by He I photons a very well defined cut-off is found at $E_{max} = 16.2$ eV (see fig. 7) which defines emission from the Fermi level. Using alkali covered W(110) the deexcitation of He* occurs via Auger deexcitation which is a "one-electron" process like UP emission. The maximum kinetic energy is

$$E_{max} = E^* - \phi,$$

where E^* is the effective excitation energy of the metastable atom in front of the surface. E_{max} defines the position of the Fermi level ($E_B = 0$). E_{max} is found to be 1.4 eV smaller than for UPS with He I ($h\nu = 21.2$ eV); this value is equal to the difference between $h\nu$ and $E^*(2\,^3S) = 19.8$ eV.

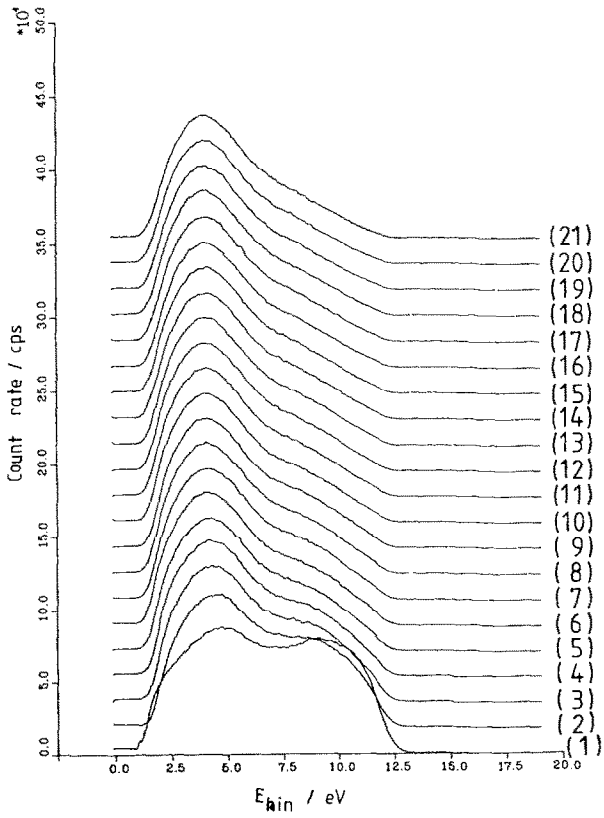

Fig. 2. He*-MIE spectra for W(110) exposed to H_2. (1) Clean W(110), (2)–(21) H_2-covered W(110), 0.5–10 L H_2 in steps of 0.5 L.

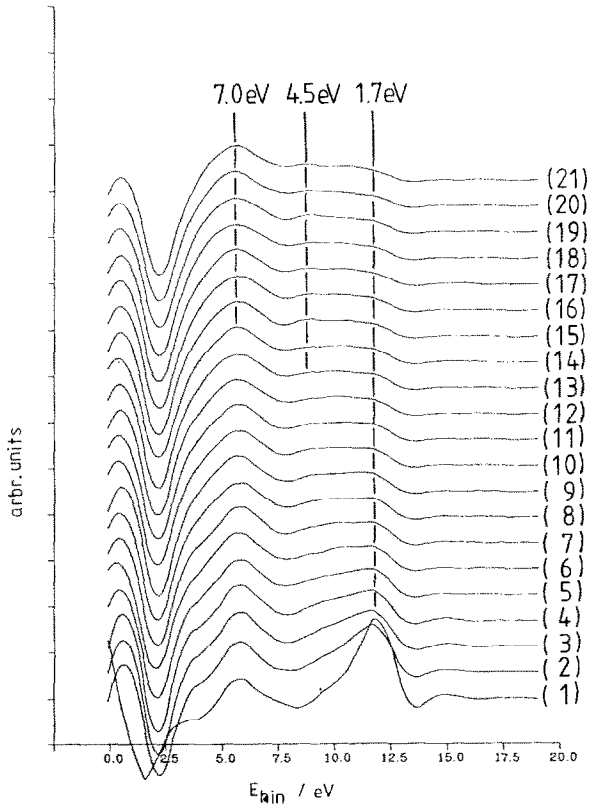

Fig. 3. Approximate deconvolution (first derivative) of the He* spectra from the clean and H_2 exposed W(110) of fig. 1.

3.1. Hydrogen on clean W(110)

Fig. 2 shows AN spectra obtained for a W(110) surface subjected to hydrogen exposures between 0 and 10 L. The spectra have been recorded in steps of 0.5 L starting with clean W(110) (1). Fig. 3 displays the results of the deconvolution which mainly reflect the SDOS [8]. The SDOS exhibits two peaks at $E_B = 1.7$ and 7.0 eV. A shoulder appears around $E_B = 4.5$ eV and becomes more pronounced with increasing hydrogen exposure (all binding energies with respect to the Fermi level). These structures are believed to correspond to the peaks at $E_B = 2.2$ and 7.0 eV seen in the UP spectrum of fig. 7b. The peak at 1.7 eV decreases and finally disappears under H exposure. The peak at $E_B = 7.0$ eV increases with increasing hydrogen exposure. These results are in close agreement with those for hydrogen adsorption on polycrystalline tungsten by Sesselmann et al. [9].

3.2. Cs on clean W(110)

Fig. 4a displays a series of MIES spectra recorded at various Cs coverages on W(110). For the clean target (curve (1) of fig. 4a) He* deexcitation occurs by AN (see fig. 2). Up to a coverage of $\theta_{Cs} = 0.18$ ML the spectra display contributions from both AN and AD. This demonstrates once more [7] the possibilities of He* serving as a local probe to distinguish between Cs and bare W substrate sites which are obviously characterized by different deexcitation mechanisms. It is necessary to keep in mind that at this coverage the macroscopic work function has already decreased by about 2 eV [1,10]. At coverages $\theta_{Cs} > 0.18$ ML the spectra are essentially governed by two features (curves (6) to (12)) :

(i) the Cs-induced feature (P_3) near E_F originates from ionization of the Cs(6s) level by He($2\,^3S$) atoms. It appears for the first time at $\theta_{Cs} \approx 0.4$ ML and grows rapidly in intensity with

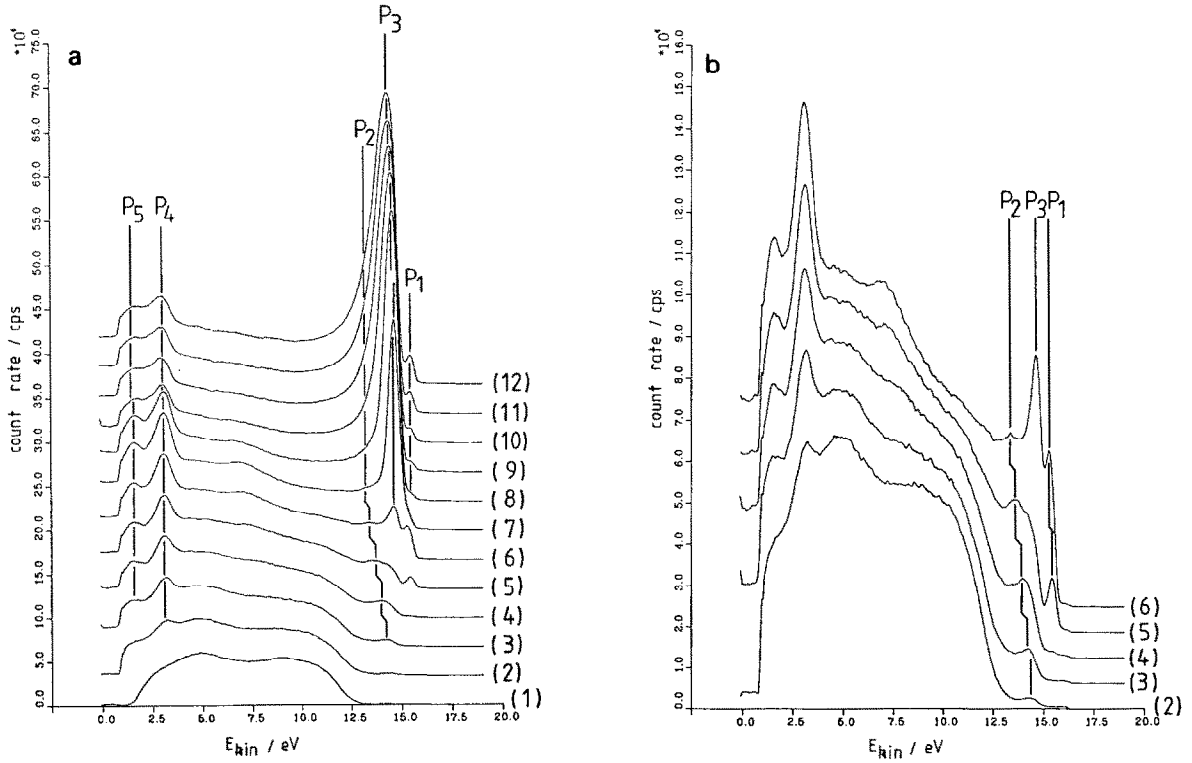

Fig. 4. He*-MIE spectra for clean and Cs-covered W(110). (a) (1) Clean W(110), (2)–(12) Cs-covered W(110), 0.09–1 ML Cs in steps of 0.09 ML; (b) details for the range: 0.09–0.45 ML (corresponds to (2)–(6) of (a)).

increasing Cs coverage. A similar behaviour has been found previously for the K adsorption on Cu(110) [7] and K on Ni(111) [11]. Beyond θ_{Cs} = 0.64 ML (corresponding to ϕ_{min}) the peak height remains approximately constant, but its width still increases considerably. The weak structure (P_1) at still higher kinetic energies arises from singlet He* ($2\,^1S$) atoms which are not converted into triplet He* ($2\,^3S$) prior to deexcitation. P_1 appears already at lower coverages than P_3 although the metastable beam consists of He($2\,^3S$) atoms mainly. Even before the appearance of the Cs(6s) derived peaks (P_1 and P_3) we see Cs induced changes ($\theta_{Cs} \geq 0.05$ ML) (P_2). Details of the emission in this coverage range are shown in fig. 4b (curves (2) to (6) of fig. 4a e.g. θ_{Cs} = 0.09–0.54 ML). Similar emission has been seen both for K on Ni(111) and Cu(110) [7,11]. Lee et al. [11] have proposed that P_2 orginates from AD involving the W(5d) electrons. We follow this interpretation for the following reasons:

- P_2 and P_3 appear together over an extended region of coverages (up to about 0.25 ML),
- the positions of P_2 and P_3 are different,
- P_2 and P_3 exhibit a different dependence on hydrogen exposure (see section 3.3).

(ii) the peaks P_4 and P_5 at E_B = 11.5 and 13 eV are due to the ionization of the Cs($5p_{3/2}$) and Cs($5p_{1/2}$) levels by He($2\,^3S$) atoms [12,13]. These levels are clearly discernible long before Cs(6s) emission occurs. The 5p intensities decrease relative to the 6s intensity as soon as the Cs(6s) ionization becomes important (see fig. 6).

Fig. 6 depicts the intensities for the Cs($5p_{3/2}$) (P_4) and the Cs(6s) (P_3) emission versus Cs coverage (a) without and (b) with hydrogen precoverage. The evaluation of the 5p intensities should be considered with caution because the background

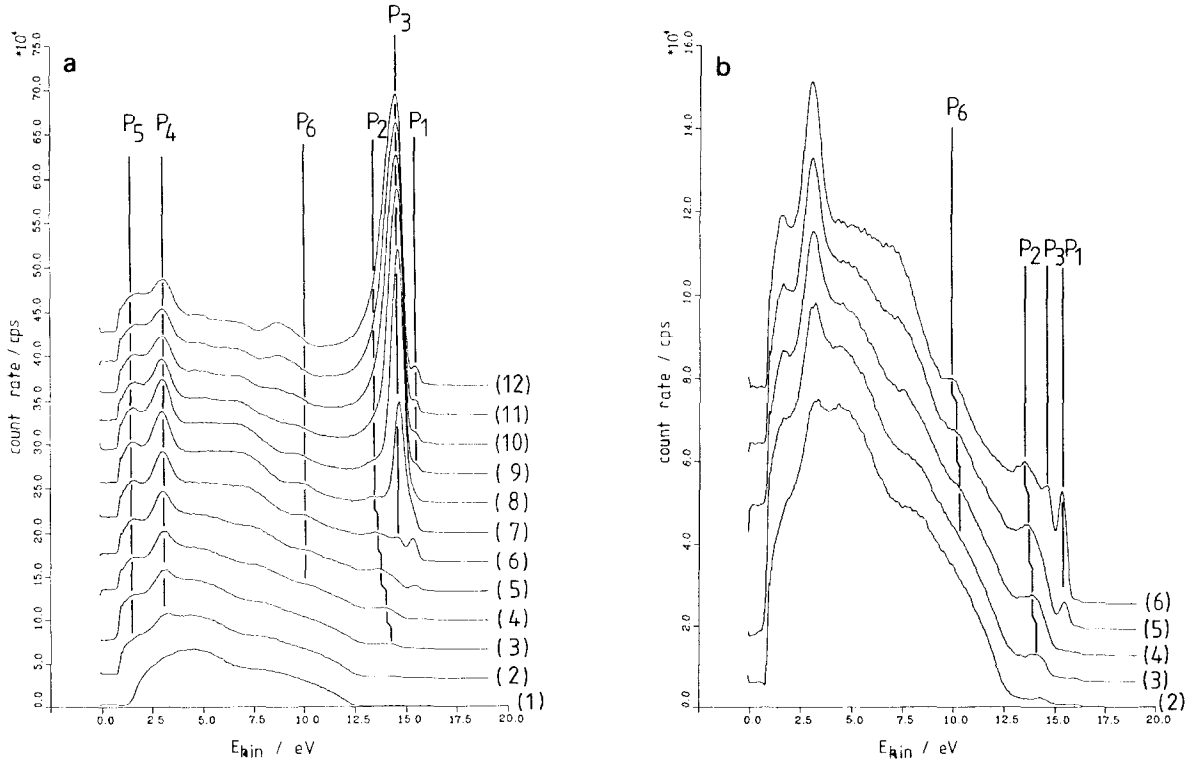

Fig. 5. He*-MIE spectra for hydrogen precovered W(110) (10 L H_2 corresponding to θ_H = 1) and subjected to Cs exposure. (a) (1) 10 L H_2 on W(110), (2)–(12) Cs-adsorption, 0.09–1 ML Cs in steps of 0.09 ML; (b) details for the range: 0.09–0.45 ML (corresponds to (2)–(6) of (a)).

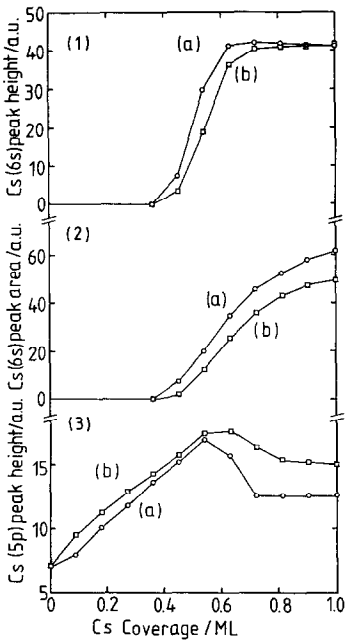

Fig. 6. Cs (6s) peak height (1), Cs (6s) peak area (2) and Cs($5p_{3/2}$) peak height (3) as a function of the Cs coverage for, (a) clean W(110), (b) H covered W(110), 10 L H_2 ($\theta_H = 1$).

subtraction is not unambiguous. Within the error margins the 5p intensity rises linearly with θ_{Cs}, e.g. proportional to the number of adsorbed Cs atoms, up to that coverage where the Cs(6s) emission becomes important. On the other hand, the Cs(6s) peak intensity starts at about 0.4 ML and rises with the coverage up to about 0.6 ML. The Cs(6s) peak area (b) increases even for coverages $\theta_{Cs} >$ 0.64 ML.

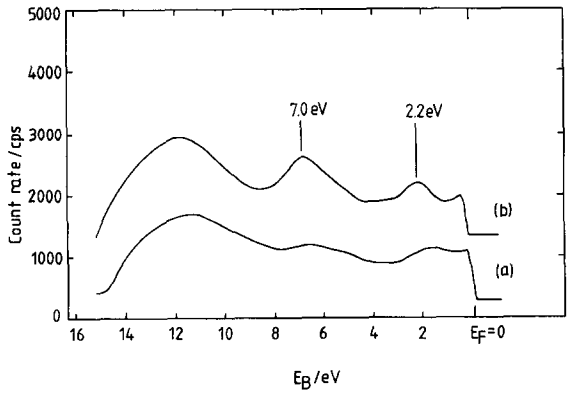

Fig. 7. HeI-UP spectra of W(110) (a) clean surface, (b) substrate exposed to 10 L H_2.

3.3. Cs on hydrogenated W(110)

Fig. 5a contains a series of AD spectra for the W(110) surface saturated with hydrogen (exposure 10 L H_2) versus the Cs coverage. Even in spite of a background pressure in the 10^{-11} Torr range (before turning the He* beam on) oxygen induced features appear between $E_B = 6.0$ and 9.5 eV (see curve (12)) [14]. They are more pronounced in fig. 5 than in fig. 4 because of the time required for the hydrogen adsorption. At Cs coverages below 0.15 ML the spectra depicted in figs. 4 and 5 show considerable differences: AN is still effective, and the AN spectra with and without adsorbed hydrogen differ in the region of the W(5d) emission (see fig. 2). Above $\theta_{Cs} = 0.27$ ML the spectra become rather similar indicating that in both situations Cs forms the toplayer, and the charge clouds of neighboring Cs atoms shield the substrate efficiently.

There are two hydrogen induced features which will be discussed in somewhat more detail (see also fig. 5b):

(a) P_2 is smaller when hydrogen is preadsorbed.

(b) There is an additional peak P_6 at $E_B = 4.7$ eV which is clearly visible as long as the substrate emission (P_2) is visible. Details of the spectra are shown in fig. 5b for the Cs coverage range up to 0.54 ML. The hydrogen induced feature can clearly be distinguished from the oxygen induced feature at $E_B = 6.3$ eV which appears at a Cs coverage of about 0.8 ML for the first time. While hydrogen atoms can be detected with extremely high sensitivity in the AN spectra, the AD spectra obtained in the presence of small amounts of Cs can thus serve to identify the adsorbed species. It is in particular possible to distinguish hydrogen from adsorbed oxygen which produces a prominent peak at $E_B = 6.3$ eV for small oxygen exposures in the AD spectra [8,14].

The Cs(6s) peak appears at slightly higher coverages in case of hydrogen preadsorption compared to adsorption on the bare substrate for all

studied coverages between 0 and 20 L H_2 (see fig. 6). The Cs(6s) peak area, which depends upon the amount of charge in the Cs surface valence band, is lower for all studied hydrogen precoverages (25% at 1 ML). The Cs(5p) peak area is smaller without hydrogen preadsorption. This is valid for all studied hydrogen precoverages (0 to 10 L H_2).

4. Discussion

Hydrogen adsorption strongly influences the SDOS of W(110). A decrease of the SDOS in the region of the Fermi level is accompanied by an increase near $E_B = 4.7$ eV which has been attributed to H–metal bond formation [9]. As can be seen from fig. 6 the Cs(6s) emission intensity is lower in the case of hydrogen and Cs coadsorption.

Fig. 6 compares the Cs(6s) and Cs(5p) emission intensities, (a) without and, (b) with hydrogen preadsorption. The onset of the Cs(6s) emission occurs around $\theta_{Cs} = 0.4$ ML while the position of ϕ_{min} is found at $\theta_{Cs} = 0.64$ ML [1,10]. This indicates that the Cs(6s) emission does not necessarily signal the beginning of the metallization of the adlayer. The 5p intensities decrease as soon as the Cs(6s) ionization becomes important. Exactly this behaviour is expected due to the shielding of the 5p electrons by the 6s electrons. This suggests that the 6s state is only weakly populated for $\theta_{Cs} < 0.4$ ML. While the Cs(6s) intensity is smaller in case of hydrogen precoverage, the opposite is valid for the 5p intensities. The width of the Cs(6s) peak at Cs saturation is also smaller when hydrogen is adsorbed previously.

Our results have to be discussed in the light of the remarkable work function changes observed by Papageorgopoulos [1] upon hydrogen preadsorption: the WF minimum $\delta\phi_{min}$ found at a Cs coverage of 0.64 ML on W(110) shifts towards smaller Cs coverages upon hydrogen preadsorption and occurs already at 0.32 ML for the surface saturated with hydrogen (10 L). Results of our group fully support these findings [15]. The saturation value $\delta\phi_{max}$ reached at $\theta_{Cs} = 1$ ML increases with increasing H precoverage, even beyond the bulk value of 2.1 eV. As proposed by Papageorgopoulos [1] the Cs deposition on hydrogen covered surfaces obviously forms an independent layer above the H layer. The main effect of the preadsorbed hydrogen seems to be an increase of the W–Cs layer distance causing an increase of the initial dipole moment. The shift and the decrease of the work function minimum (ϕ_{min}) with H precoverage can be explained in this manner [16]. Our results support this view in all aspects.

However, the WF dependence, especially its change upon hydrogenation, does not reflect itself in the MIE spectra. In particular the remarkable shift of ϕ_{min} from 0.64 to 0.32 ML is not reflected. In contrast to the conclusions of Papageorgopoulos we find no evidence for an increase in the electron density of the Cs valence band which should manifest itself in an increase of the Cs(6s) peak area when hydrogen is preadsorbed. Within the accuracy of the measurements the position of ϕ_{min} and the onset of the Cs(6s) ionization coincide which is not the case for the Cs adsorption alone. It is generally believed that the position of ϕ_{min} is correlated with the beginning metallization of the Cs adlayer. For the particular case of coadsorption of hydrogen and Cs on W(110) indeed the Cs(6s) ionization is not visible before the metallization of the adlayer starts. From the intensities for 5p and 6s emission with and without hydrogen preadsorption we conclude that the shift of ϕ_{min} and the increase of ϕ_{max} upon hydrogen preadsorption cannot be explained by an increase of the electron density of the Cs overlayer.

An alternate explanation of the work function changes upon coadsorption of alkali and foreign atoms has been offered by Burt and Heine [17]. The difference of the work function of cesium bulk material and a cesium film is caused by the different boundary conditions imposed on the conduction electrons. The Fermi wavelength of the conduction electrons becomes comparable to the dimensions of the confinement. This size effect changes the kinetic energy of the electrons and hence the Fermi energy thus causing an equivalent change of the work function.

A similar effect may occur after hydrogen preadsorption on W(110): the H-preadsorption raises the Cs substrate distance [1] and hence the Cs substrate interaction. The lowered binding may

impose different boundary conditions on the conduction electrons.

5. Summary

We have applied metastable impact electron spectroscopy to the study of the coadsorption of hydrogen and cesium on W(110). Adsorption of hydrogen alone leads to a reduction of the SDOS near the Fermi level which is accompanied by the formation of a H–metal bond at $E_B = 4.7$ eV.

Adsorption of Cs on W(110) leads to the formation of the Cs(6s) band at the Fermi level. Ionization of Cs(6s) starts at a Cs coverage of 0.4 ML. In the coverage range between 0.3 and 0.5 ML a small peak orginating from AD involving W(5d) electrons is seen.

Adsorption of Cs on hydrogen precovered W(110) leads to similar features, but the intensity of the Cs(6s) emission is reduced by 25%. In addition the formation of a H(1S)–metal bond resonance is seen at $E_B = 4.7$ eV in the range from 0.3 to 0.5 ML. The lowering of the work function minimum due to the hydrogen preadsorption observed by Papageorgopoulos can be explained by the increased Cs layer–substrate distance.

The shift of the work function minimum and the increase of the saturation value of the work function due to the hydrogen preadsorption is not fully understood yet; no increase of the density of electrons in the Cs valence band – as has been proposed by Papageorgopoulos – can be observed.

Acknowledgement

Financial support by the Bundesministerium für Forschung und Technologie and the Deutsche Forschungsgemeinschaft is gratefully acknowledged.

References

[1] C.A. Papageorgopoulos, Phys. Rev. B 40 (1989) 1546.
[2] G. Ertl, Surf. Sci. 89 (1979) 525.
[3] W. Keller, H. Morgner and W.A. Müller, Mol. Phys. 58 (1986) 1039.
[4] H. Hotop, E. Kolb and J. Lorenzen, J. Electron. Spectrosc. Relat. Phenom. 16 (1979) 213.
[5] O. Leisin, H. Morgner and W. Müller, Z. Phys. A 304 (1982) 23.
[6] M. Wehrhahn, Diplomathesis TU Clausthal (1989).
[7] B. Woratschek, W. Sesselmann, J. Küppers, G. Ertl and H. Haberland, Phys. Rev. Lett. 55 (1985) 1231.
[8] W. Sesselmann, B. Woratschek, J. Küppers, G. Ertl and H. Haberland, Phys. Rev. B 35 (1987) 1547.
[9] W. Sesselmann, B. Woratschek, J. Küppers, G. Ertl and H. Haberland, Phys. Rev. B 35 (1987) 8348.
[10] W. Maus-Friedrichs, H. Hörmann and V. Kempter, Surf. Sci. 224 (1989) 112.
[11] J. Lee, C. Hanrahan, J. Arias, F. Bozso, R.M. Martin and H. Metiu, Phys. Rev. Lett. 54 (1985) 1440.
[12] B. Woratschek, W. Sesselmann, J. Küppers, G. Ertl and H. Haberland, J. Chem. Phys. 86 (1987) 2411.
[13] C.Y. Su, I. Lindau, P.W. Chye, S.-J. Oh and W.E. Spicer, J. Electron. Spectrosc. Relat. Phenom. 31 (1983) 221.
[14] W. Maus-Friedrichs, S. Dieckhoff, M. Wehrhahn and V. Kempter, Dünnschichttechnologien '90, Band I, VDI-Verlag GmbH Düsseldorf, 123 (1990).
[15] H. Brenten, H, Müller, D. Kruse and V. Kempter, to be published.
[16] J.P. Muscat and I. Batra, Phys. Rev. B 34 (1986) 2889.
[17] M.G. Burt and V. Heine, J. Phys. C 11 (1978) 961.